

Supporting information

Manipulating cellular activities using an ultrasound-chemical hybrid tool

Ching-Hsiang Fan^{1,6}, Yao-Shen Huang^{2,6}, Wei-En Huang^{3,6}, Albert Alexander Lee^{4,6}, Sheng-Yang Ho⁴, Yu-Lin Kao², Cuei-Ling Wang², Yen-Ling Lian², Tasuku Ueno⁵, Tsung-Shing Andrew Wang⁴, Chih-Kuang Yeh¹, Yu-Chun Lin²

¹Department of Biomedical Engineering and Environmental Sciences, National Tsing Hua University, Hsinchu, Taiwan

²Institute of Molecular Medicine, National Tsing Hua University, Hsinchu, Taiwan

³Department of Life Science, National Tsing Hua University, Hsinchu, Taiwan⁴Department of Chemistry, National Taiwan University, Taipei, Taiwan

⁵Graduate School of Pharmaceutical Sciences, University of Tokyo, Tokyo, Japan

⁶These authors contributed equally to the work

To whom correspondence should be addressed:

ycl@life.nthu.edu.tw

Table of Contents

Supplementary Figures

Fig. S1. **RPB** is unable to induce dimerization events inside cells.

Fig. S2. **RPB** is a functional chemical dimerizer.

Fig. S3. Characterization of folate-conjugated, fluorescent-labeling microbubbles (FMBs).

Fig. S4. Folate-coated microbubbles (FMBs) attached to the cell membrane upon ultrasound excitation.

Fig. S5. Folate-coated microbubbles (FMBs) rapidly collapse upon ultrasound excitation.

Fig. S6. Excitation by ultrasound on microbubbles-bound cells induces sonoporation.

Fig. S7. Sonoporation does not affect the membrane phospholipid composition.

Fig. S8. Cell viability after the ultrasound excitation with different acoustic pressures.

Fig. S9. **GA₃-AM** but not **GA₃** induces dimerization events inside cells.

Fig. S10. Sonoporation triggers the **GA₃**-dependent CID system in C6 neuroblastoma cells.

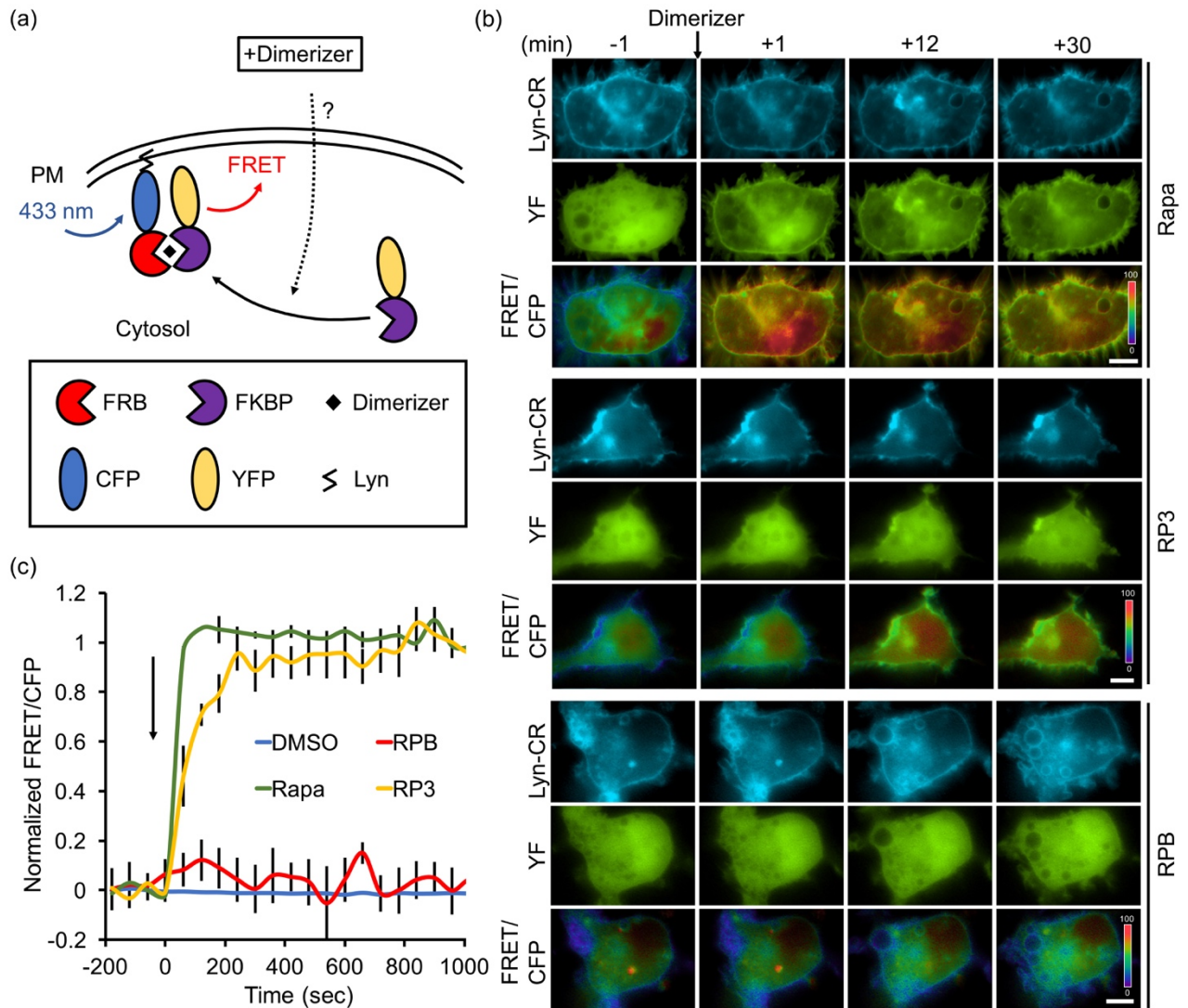
Fig. S11. Sonoporation triggers the **RPB**-dependent CID system in C2BBel cells.

Supplementary Methods

- I. Synthesis of Biotin-PEG3-alkyne
- II. Synthesis of Rapa-PEG3-N3 (RP3)
- III. Synthesis of Rapa-PEG6-Biotin (RPB)
- IV. Synthesis of GA₃-AM

Supplementary References

Supplementary Figures



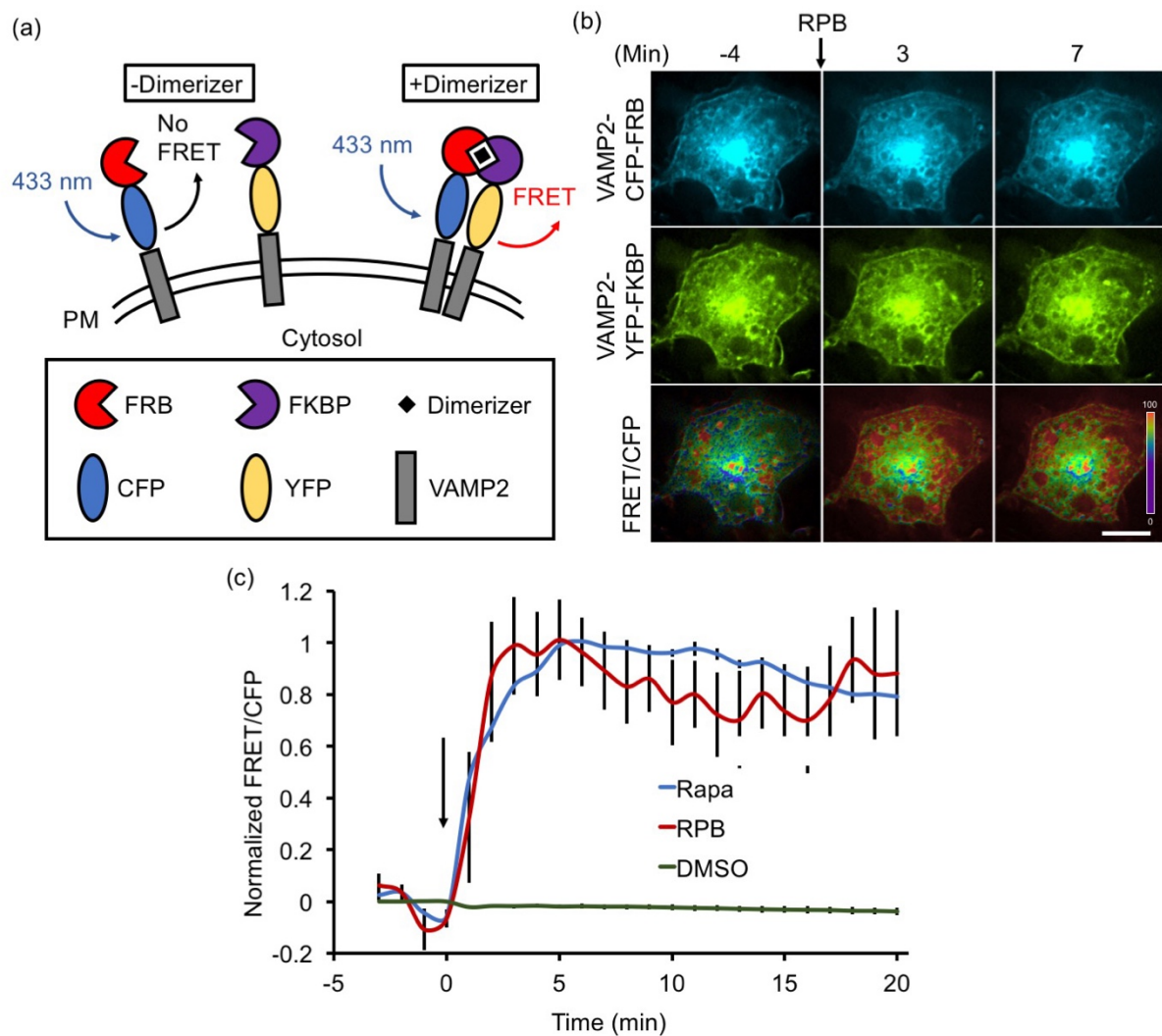


Figure S2. RPB is a functional chemical dimerizer. (a) Schematic of an experiment evaluating whether chemical dimerizers induce dimerization events. The functional dimerizers can induce the dimerization between VAMP2-CFP-FRB and VAMP2-YFP-FKBP on the cell surface and, therefore, increase the FRET signal. (b) The addition of **RPB** (50 nM) rapidly induces the FRET signal between VAMP2-CFP-FRB and VAMP2-YFP-FKBP on the cell surface. Scale bar= 10 μm. In addition, see Movie S2. (c) The normalized FRET/CFP ratio in cells treated with 0.1% DMSO alone, **RPB** (50 nM), or **Rapa** (50 nM) was measured at the indicated time points. Arrow indicates time point of dimerizers or DMSO treatment. Error bars represent the SEM (n=7 cells).

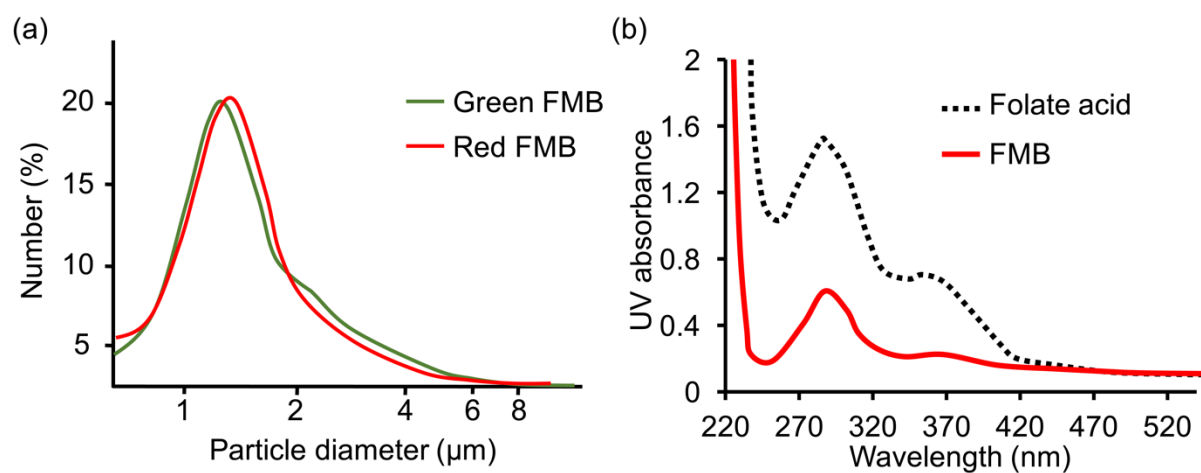


Figure S3. Characterization of folate-conjugated, fluorescent-labeling microbubbles (FMBs). (a) The mean size distribution of the green FMB and red FMB were $1.4 \pm 0.2 \mu\text{m}$ and $1.5 \pm 0.2 \mu\text{m}$, respectively. The mean concentration of the green FMB and red FMB were $(11.5 \pm 0.6) \times 10^9 \text{ MBs/mL}$ and $(7.4 \pm 1.5) \times 10^9 \text{ MBs/mL}$, respectively. (b) Spectrophotometer results. Folate and FMBs showed UV absorption wavelengths at 290 nm.

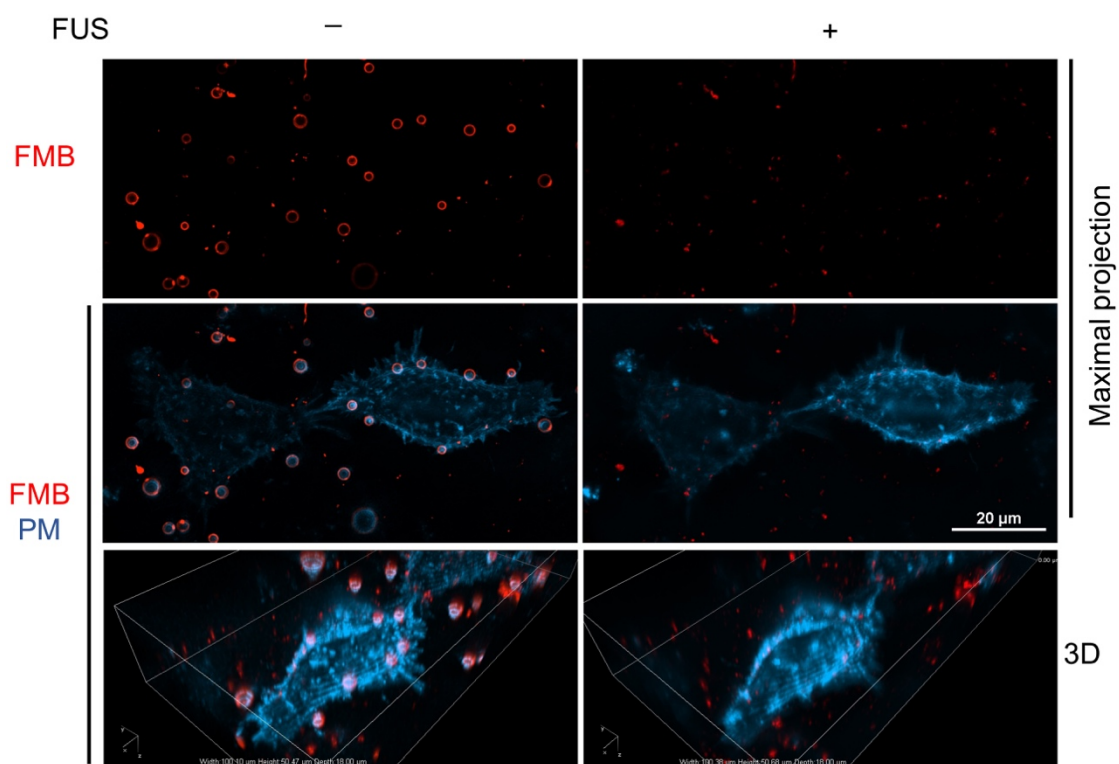


Figure S4. Folate-coated microbubbles (FMB) attached to the cell membrane upon ultrasound excitation. HeLa cells expressing Lyn-CFP (a plasma membrane marker, PM) were incubated with red FMBs, followed by ultrasound excitation (1-MHz, 0.5 MPa, 500 cycles, 0.1 Hz PRF, 5 sec sonication duration). In addition, see Movie S3. Note that strong signal of red FMBs can also be observed with CFP channel due to the fluorophore bleed-through of DiI dye to the CFP channel.

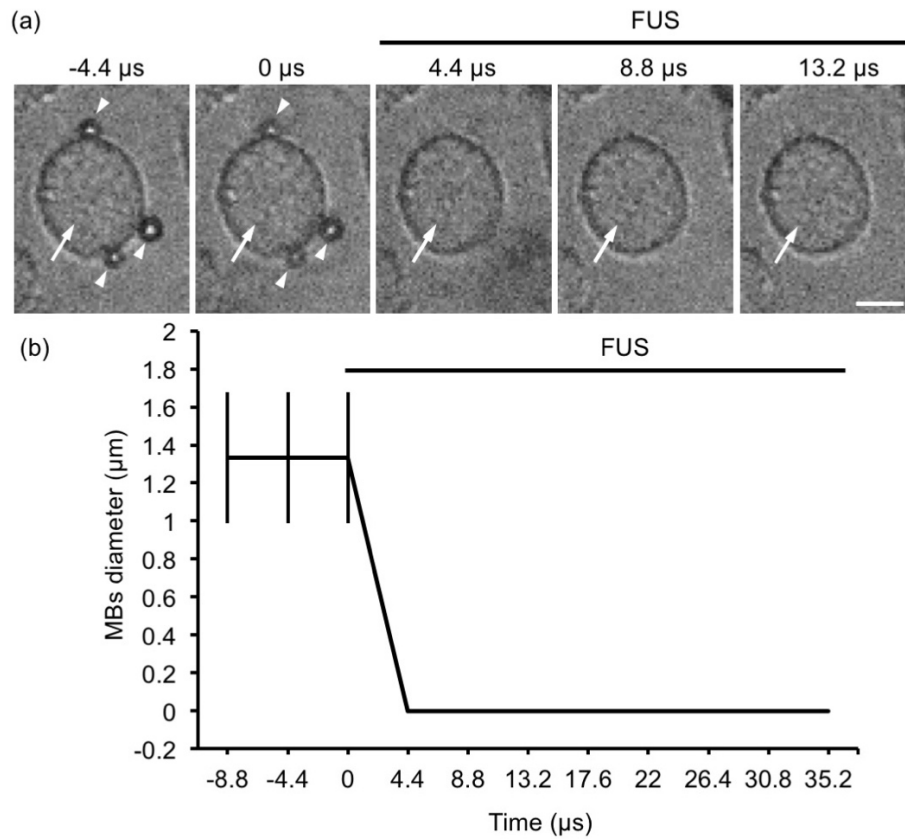


Figure S5. Folate-coated microbubbles (FMBs) rapidly collapse upon ultrasound excitation. (a) HeLa cells (arrows) were incubated with FMBs (arrowheads) and then excited by ultrasound (1 MHz, 0.5 MPa, 500 cycles, 0.1 Hz PRF, 5 sec sonication duration). The realtime behavior of microbubbles was imaged by acousto-optical system, which allowed for concurrent ultrasound sonication and high-speed bright field imaging. Scale bar = 2 μm. In addition, see Movie S4. (b) The average diameter of microbubbles was measured at the indicated time points. Error bars represent the Standard deviation (n=6).

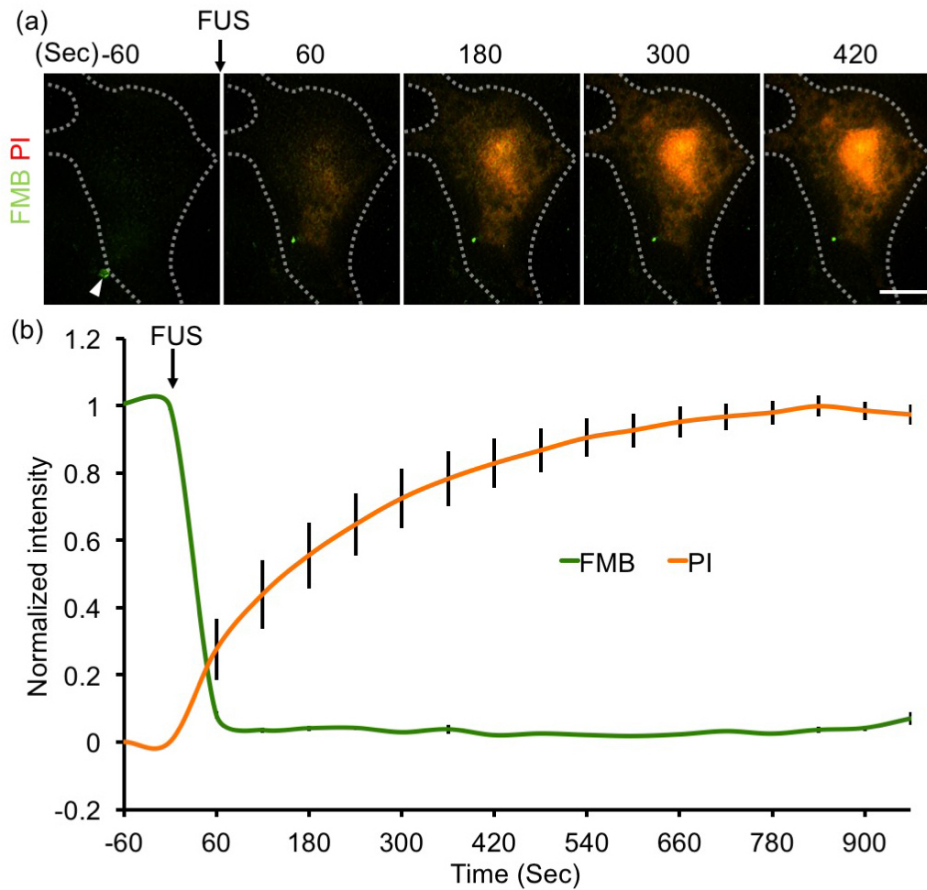


Figure S6. Excitation by ultrasound on microbubbles-bound cells induces sonoporation. (a) Green FMB (arrowhead)-bound HeLa cells were excited by a short pulse of ultrasound in the presence of the membrane impermeable dye Propidium Iodide (PI, 100 μ M). The cell boundary is highlighted by the dotted lines. The excitation by the ultrasound rapidly disrupted the green FMBs, which was accompanied by an increase in the PI intensity in the cytosol. Scale bar=10 μ m. In addition, see Movie S5. (b) The normalized fluorescence intensity of the membrane-bound green FMBs (n=30) and PI in the cytosol (n=13) was measured at the indicated time points. Error bars represent the SEM.

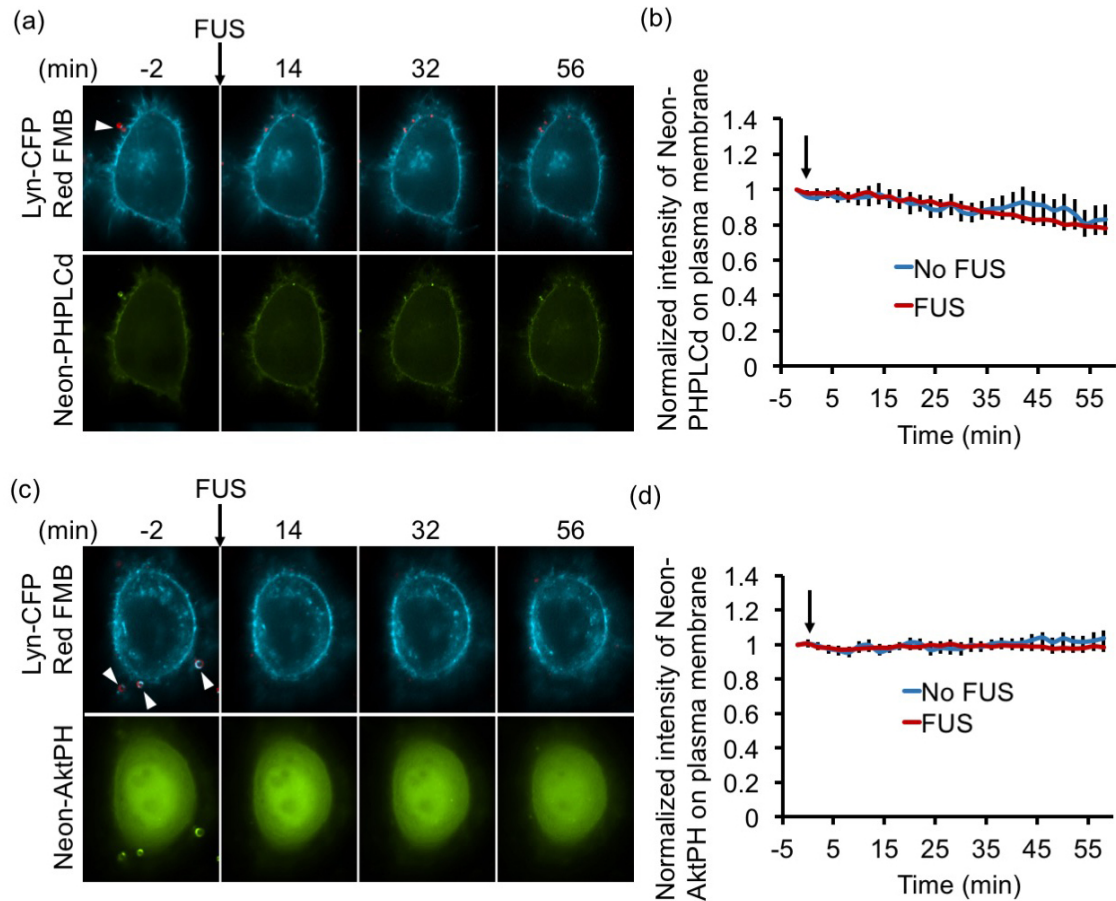


Figure S7. Sonoporation does not affect the membrane phospholipid composition. (a)(c) The level of PIP₂ and PIP₃ in the cell membrane was visualized by specific biosensors, Neon-PHPLCd and Neon-AktPH, respectively, upon sonoporation. Arrowheads mark the red FMBs. The plasma membrane was labeled with Lyn-CFP protein. Scale bar=10 μ m. In addition, see Movie S6. (b)(d) The level of Neon-PHPLCd (b) and Neon-AktPH (d) in the plasma membrane upon sonoporation was quantified. Error bars represent the SEM (n>6 cells). Note that strong signal of red FMBs can be also observed with CFP and YFP channel due to the fluorophore bleed-through of DiI dye to the CFP and YFP channel.

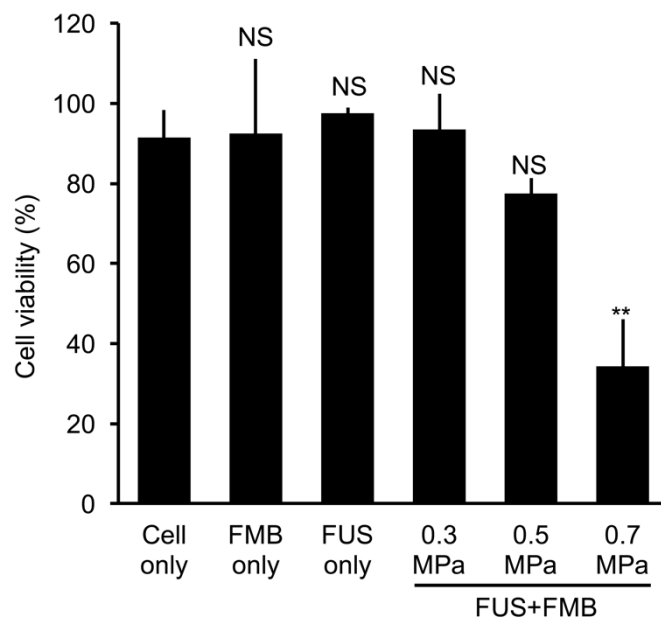


Figure S8. Cell viability after the ultrasound excitation with different acoustic pressures. Quantification data of the MTT assay, which tests the cell viability after excitation by ultrasound with acoustic pressures ranging from 0.3 MPa to 0.7 MPa. The cell viability was determined at 24 hours after indicated treatments with Alamar Blue. Error bars represent the SEM from three independent experiments. NS and ** represent no significant differences and $P < 0.01$, respectively, between the control and indicated group).

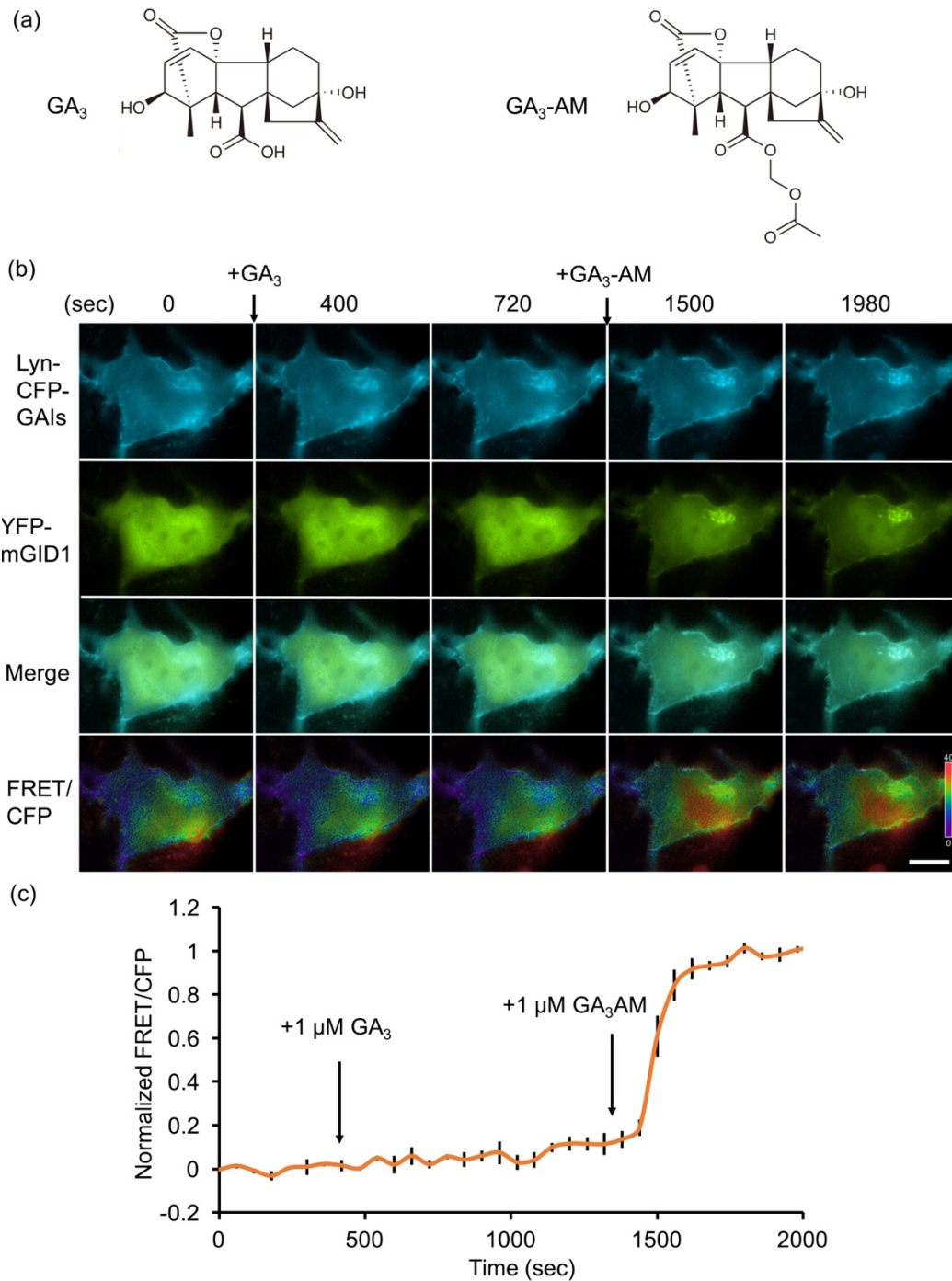


Figure S9. $\text{GA}_3\text{-AM}$ but not GA_3 induces dimerization events inside cells. (a) Chemical structure of GA_3 and $\text{GA}_3\text{-AM}$. (b) COS7 cells expressing membrane-anchoring Lyn-CFP-GAIs and cytosolic YFP-mGID1 were treated with GA_3 ($1 \mu\text{M}$) and $\text{GA}_3\text{-AM}$ ($1 \mu\text{M}$) in tandem. Scale bar= $10 \mu\text{m}$. In addition, see Movie S9. (c) The normalized FRET/CFP ratio in cells treated with GA_3 and $\text{GA}_3\text{-AM}$ at the indicated time points. Error bars represent the SEM ($n=8$ from two independent experiments).

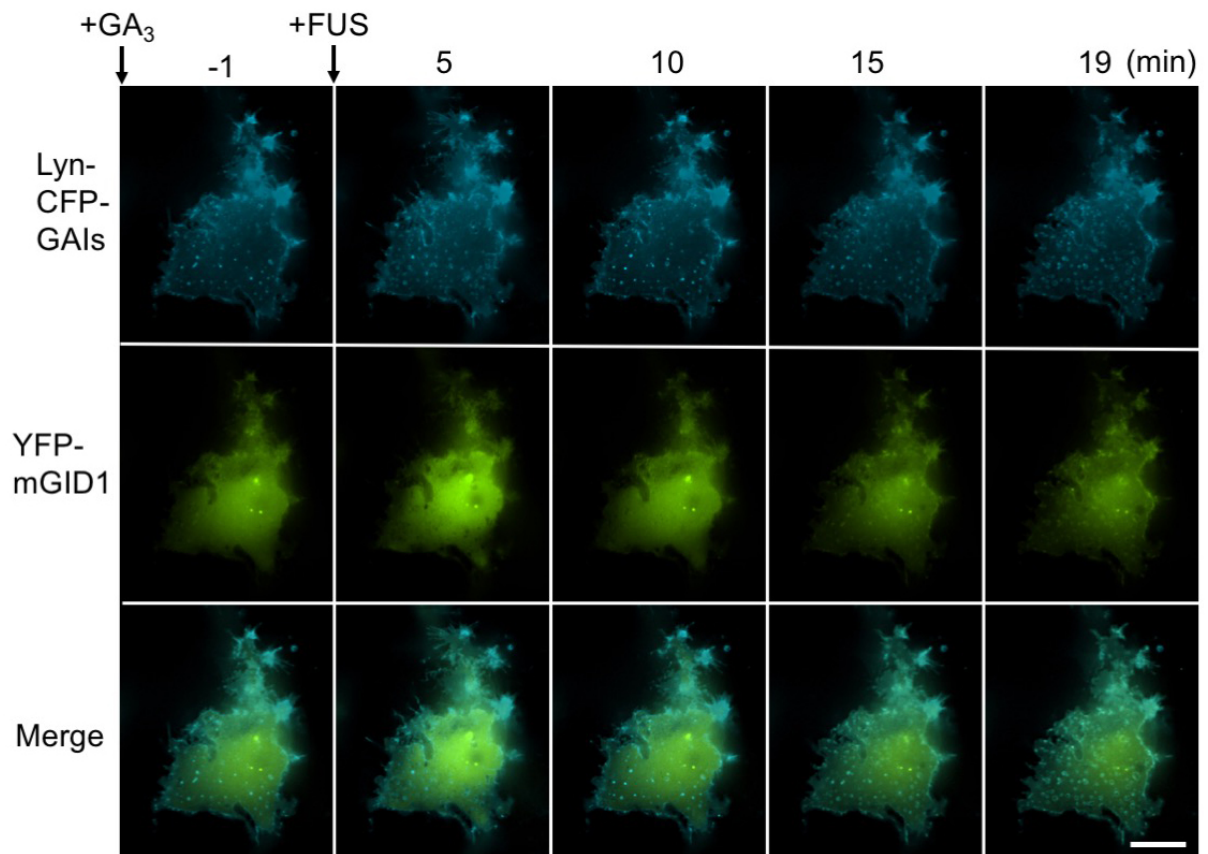


Figure S10. Sonoporation triggers the **GA₃**-dependent CID system in C6 neuroblastoma cells. C6 cells expressing membrane-anchoring Lyn-CFP-GAIs and cytosolic YFP-mGID1 were incubated with FMBs in the presence of **GA₃** (1 mM). The excitation by the ultrasound induced the translocation of YFP-mGID1 to the plasma membrane, which was accompanied by an elevation in the FRET signal. In addition, see Movie S12. Scale bar: 20 μ m. In addition, see Movie S11.

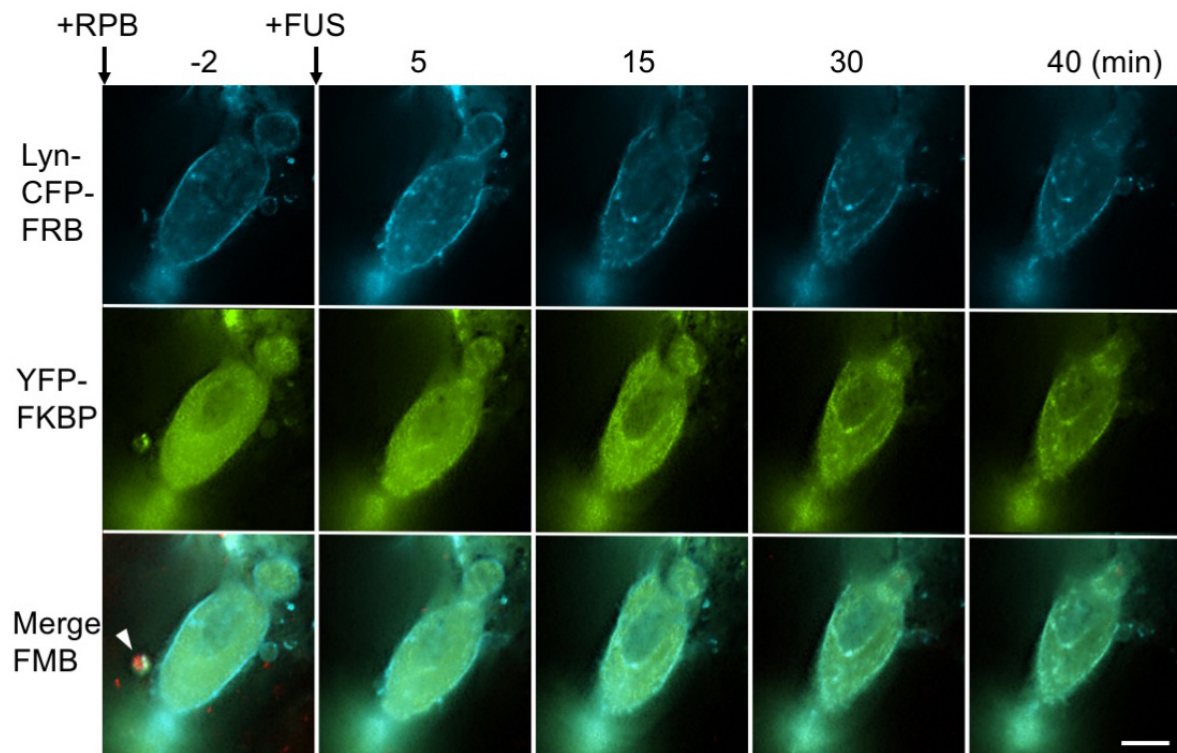
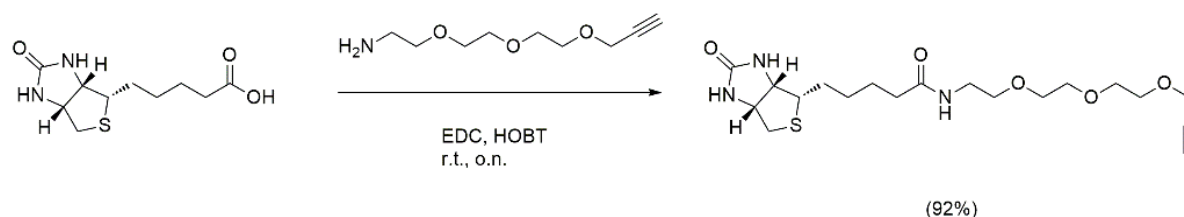


Figure S11. Sonoporation triggers the **RPB**-dependent CID system in C2BBe1 cells. C2BBe1 expressing membrane-anchoring Lyn-CFP-FRB and cytosolic YFP-FKBP were incubated with red FMBs in the presence of RPB (50 nM). The excitation by the ultrasound induced the translocation of YFP-FKBP to the plasma membrane, which was accompanied by an elevation in the FRET signal. Scale bar: 20 μ m. In addition, see Movie S13. Note that strong signal of red FMBs can be also observed with CFP and YFP channel due to the fluorophore bleed-through of DiI dye to the CFP and YFP channel.

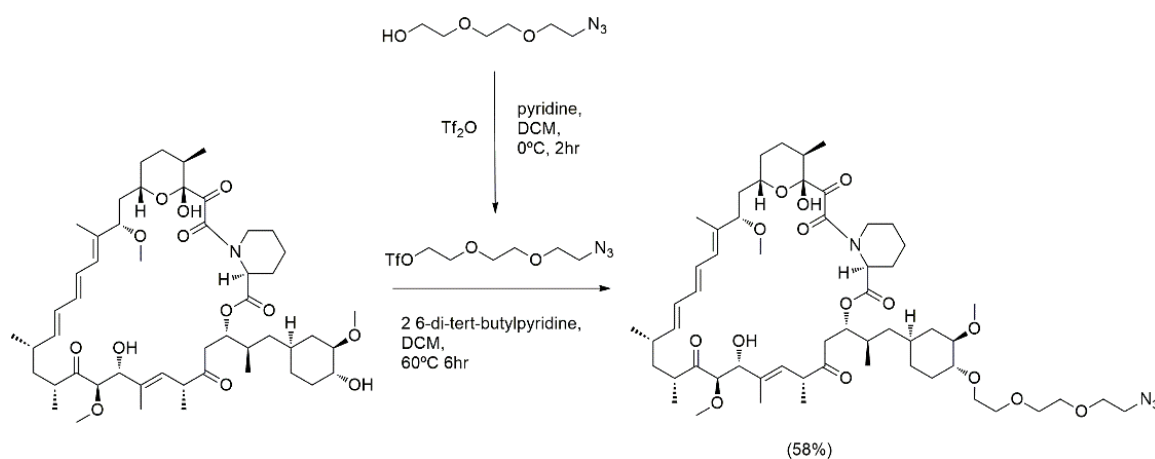
Supplementary Methods

Synthesis of Biotin-PEG₃-alkyne



3-(2-(2-(2-aminoethoxy)ethoxy)ethoxy)prop-1-yne (H₂N-PEG₃-alkyne) was synthesized as previously described.¹ EDC (288 mg, 1.50 mmole) and HOBT (202 mg, 1.49 mmole) were added to a solution of Biotin (244 mg, 1.00 mmole) in dry DMF (12 mL), and the solution was stirred at room temperature for 30 min. Then, the reaction mixture was mixed with 3-(2-(2-(2-aminoethoxy)ethoxy)ethoxy)prop-1-yne (187 mg, 1.00 mmole) and stirred at room temperature overnight. Upon the completion of the reaction, the reaction was concentrated to dryness and purified by flash column chromatography (DCM/MeOH = 10/1) to obtain **Biotin-PEG₃-alkyne** as a white solid (380 mg, 0.92 mmole, 92%)¹. H-NMR (400 MHz, CDCl₃): δ 6.86 (1 H, t, $J = 4.7$ Hz), 6.82 (1 H, br), 5.72 (1 H, br), 4.48 (1 H, dd, $J = 4.4, 7.7$ Hz), 4.29 (1H, dd, $J = 4.6, 7.8$ Hz), 4.17 (2H, d, $J = 2.4$ Hz), 3.63 (8H, m), 3.54 (2 H, t, $J = 5.0$ Hz), 3.40 (2 H, m), 3.11 (1 H, m), 2.87 (1 H, dd, $J = 4.9, 12.8$ Hz), 2.71 (1 H, d, $J = 12.8$ Hz), 2.44 (1 H, t, $J = 2.4$ Hz), 2.21 (2 H, t, $J = 7.5$ Hz), 1.67 (4 H, m), 1.41 (2 H, m). ¹³C-NMR (100 MHz, CDCl₃): δ 173.43, 164.26, 79.32, 74.80, 70.09, 69.94, 69.72, 69.66, 68.79, 61.57, 60.02, 58.11, 55.60, 40.29, 38.86, 35.69, 28.17, 27.87, 25.44. HRMS (ESI⁺): calculated for [M+Na]⁺, 436.1882; found, 436.1895.

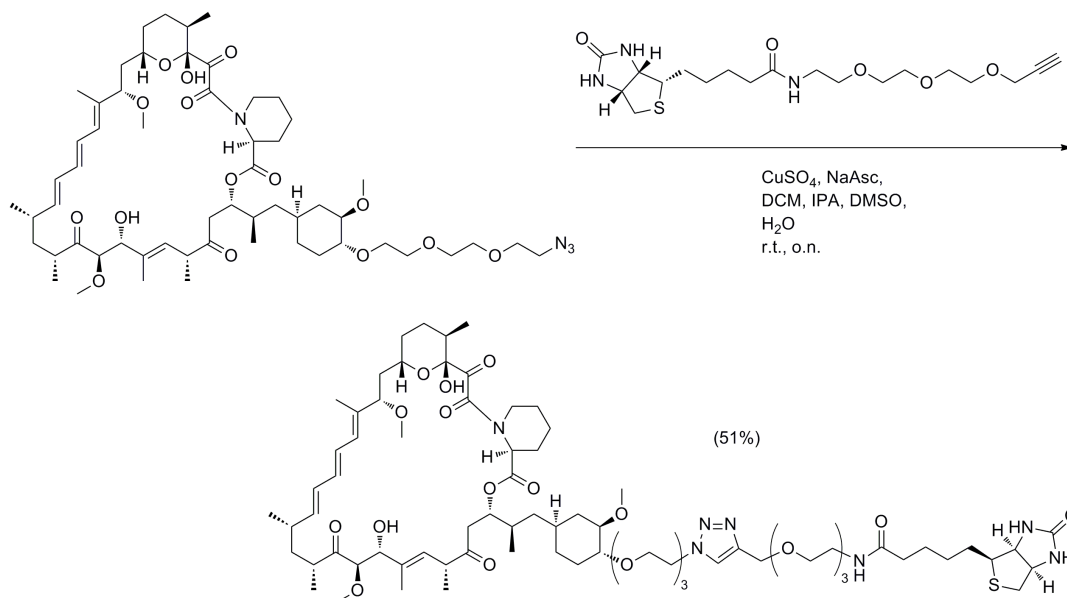
Synthesis of Rapa-PEG₃-N₃ (RP3)



2-(2-(2-azidoethoxy)ethoxy)ethanol (HO-PEG₃-N₃) was synthesized as previously described². 2-(2-(2-azidoethoxy)ethoxy)ethanol (284 mg, 1.62 mmole) was dissolved in dry DCM (15 mL) and cooled to 0°C in an ice bath. Subsequently, 2,6-ditertbutylpyridine (370 μ L) and trifluoromethanesulfonic anhydride (340 μ L, 2.02 mmole) were added to the reaction. The reaction was stirred at 0°C for 2 hr. After dilution with

DCM, the organic layer was washed with 10% HCl, brine, and water. The organic layer was recovered, dried over MgSO₄, filtered, and evaporated to dryness. The residual oil was dissolved in dry DCM (5 mL), and **Rapa** (120 mg, 0.13 mmole) and 2,6-di-*tert*-butylpyridine (500 μL) were added to the solution. The reaction was heated to 60°C and stirred overnight. When **Rapa** could no longer be detected by TLC, the reaction was diluted with DCM and washed with 10% HCl, brine, and water. The organic layer was recovered, dried over MgSO₄, filtered, and evaporated to dryness. The purification was carried out by flash column chromatography (HEX/EA = 1/1) to obtain **Rapa-PEG₃-N₃** as a white solid (81 mg, 0.076 mmole, 58%). ¹H-NMR (500 MHz, CDCl₃): δ 6.34(2 H, m), 6.12 (1 H, m), 5.95 (1 H, d, *J* = 9.8 Hz), 5.50 (1 H, m), 5.40 (1 H, d, *J* = 10.0 Hz), 5.27 (1 H, m), 5.14 (1 H, m), 4.78 (1 H, s), 4.16 (1 H, d, *J* = 5.7 Hz), 3.72 (3 H, m), 3.65 (10 H, m), 3.56 (2 H, m), 3.44 (3 H, s), 3.38 (3 H, m), 3.32 (3 H, s), 3.12 (3 H, s), 3.07 (2 H, m), 2.07 (2 H, m), 2.56 (1 H, m), 2.30 (1 H, m), 1.96 (6 H, m), 1.80-0.60 (41 H, m). ¹³C-NMR (125 MHz, CDCl₃): δ 215.53, 208.22, 192.56, 169.22, 166.74, 140.14, 135.99, 135.49, 133.63, 130.14, 129.58, 126.68, 126.37, 98.47, 84.82, 84.37, 83.00, 77.15, 75.66, 70.98, 70.95, 70.66, 70.51, 69.98, 69.13, 67.17, 59.35, 57.74, 55.85, 51.26, 50.67, 46.54, 44.21, 41.44, 40.70, 40.20, 38.84, 38.29, 36.23, 35.10, 33.74, 33.17, 32.99, 31.71, 31.23, 29.93, 27.23, 27.05, 25.29, 21.51, 20.64, 16.23, 16.03, 15.89, 13.73, 13.16, 10.16. HRMS (ESI⁺): calculated for [M+Na]⁺, 1093.6300; found, 1093.6322.

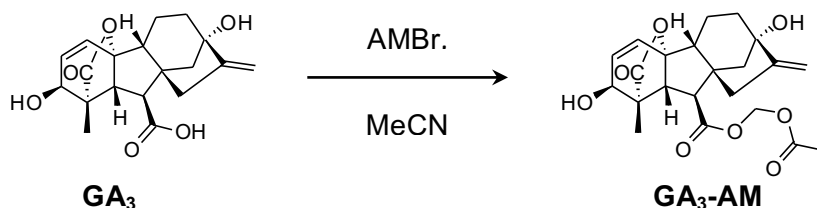
Synthesis of Rapa-PEG₆-Biotin (RPB)



The method was modified from a previous report³. **RP3** (0.1 mL of 40 mM stock dissolved in DMSO, 4.3 mg) and **Biotin-PEG₃-alkyne** (0.1 mL of 40 mM stock dissolved in DMSO, 1.7 mg) were mixed in a solution of DCM (0.2 mL), isopropanol (0.7 mL), DMSO (1.9 mL) and water (0.4 mL). Then, Copper(II) Sulfate (0.1 mL of 450 mM stock dissolved in water) and sodium ascorbate (0.2 mL of 450 mM stock dissolved in water) were added to the solution, and the reaction was stirred at room temperature overnight. The reaction was

then subjected to centrifugal evaporation and concentrated to dryness. The residual oil was dissolved in acetonitrile/water 1:1 and purified by HPLC, using a gradient eluent of 50%-100% ACN in water supplemented with 0.1% TFA on a YMC-Pack ODS-A column (250x20 mm) to obtain **Rapa-PEG₆-Biotin** as a white solid (3.0 mg, 51%). HRMS (ESI+): calculated for [M+H]⁺, 1484.8465; found, 1484.8377.

Synthesis of **GA₃-AM**



The synthesis of **GA₃-AM** has been described previously⁴. In brief, a flame-dried 50 mL round-bottomed 2-neck flask equipped with a magnetic stirring bar was charged with gibberellic acid (**GA₃**, 200 mg, 0.58 mmol), diisopropylethylamine (100 μ l) and dist. acetonitril 20 mL under an Ar atmosphere. The mixture was stirred in an ice bath for 5 min, and a solution of bromomethyl acetate (AM-Br, 55 μ l/dist. Acetonitril 10 mL) was added dropwise via a syringe. The resulting mixture was stirred in an ice bath for 1 h and then allowed to warm to an ambient temperature; the stirring was continued for 2 h. The reaction mixture was poured into a 100 mL ammonium chloride solution (5 g NH_4Cl / 100 mL H_2O) and extracted with AcOEt 3 x 30 mL. The combined organic layer was washed with brine, dried over anhydrous Na_2SO_4 , and concentrated to dryness in vacuo. The residue was purified by column chromatography to yield a colorless solid (**GA₃-AM**).

Supplementary References

- (1) Goswami, L. N., Ma, L., Chakravarty, S., Cai, Q., Jalisatgi, S. S., and Hawthorne, M. F. (2013) Discrete nanomolecular polyhedral borane scaffold supporting multiple gadolinium(III) complexes as a high performance MRI contrast agent. *Inorg. Chem.* 52, 1694–1700.
- (2) Schmidt, F., Rosnizeck, I. C., Spoerner, M., Kalbitzer, H. R., and Konig, B. (2011) Zinc(II)cyclen-peptide conjugates interacting with the weak effector binding state of Ras. *Inorganica Chim. Acta* 365, 38–48.
- (3) Umeda, N., Ueno, T., Pohlmeier, C., Nagano, T., and Inoue, T. (2011) A photocleavable rapamycin conjugate for spatiotemporal control of small GTPase activity. *J. Am. Chem. Soc.* 133, 12–4.
- (4) Miyamoto, T., DeRose, R., Suarez, A., Ueno, T., Chen, M., Sun, T., Wolfgang, M. J., Mukherjee, C., Meyers, D. J., and Inoue, T. (2012) Rapid and orthogonal logic gating with a gibberellin-induced dimerization system. *Nat. Chem. Biol.* 8, 465–70.